ASTRONOMY & ASTROPHYSICS
SUPPLEMENT SERIES

Astron. Astrophys. Suppl. Ser. **71,** 25-38 (1987)

A WSRT 21 cm deep survey of two fields in Hercules

M. J. A. Oort and H. J. van Langevelde

Sterrewacht Leiden, Postbus 9513, 2300 RA Leiden, The Netherlands

Received March 17, accepted April 22, 1987

Summary. — We present a deep 21 cm survey, carried out with the Westerbork Synthesis Radio Telescope (WSRT), of two fields in the constellation of Hercules. These areas were observed previously at 21 cm in the Leiden-Berkeley Deep Survey (LBDS), (Windhorst *et al.*, 1984), but with a factor of 3 higher noise level. A complete sample is defined, containing 116 radio sources with a peak flux above 5 σ, within the -7 dB attenuation radius (0°464). This complete sample is used to determine the 1412 MHz source counts down to 0.45 mJy. The counts from the current sample show the same small scale structure at ≈ 1 mJy as was found in previous surveys. A direct comparison is made with the LBDS observations of the same fields. It is shown that the 5 σ peak flux cut-off in the complete sample is not stringent enough to sufficiently avoid contamination by spurious sources, especially when strong ($S \geqq 100$ mJy) sources are present in the field. Finally, a search was made for the variable sources.

Key words : radio source surveys — radio source counts — radio interferometers.

1. Introductions.

Systematic deep radio surveys are an integral part in statistical studies concerning the spatial distribution of populations of radio sources. Through the years, several square degrees of the sky have been mapped with the WSRT at 21 cm down to the (sub)milliJansky level. In particular, the Leiden-Berkeley Deep Survey (Windhorst *et al.*, 1984) [LBDS], the Westerbork — Einstein Deep Survey (Katgert-Merkelijn *et al.*, 1985) [WEDS] — both with 5 σ detection limits ≈ 1 mJy, and the survey of Lynx.3A (Oort, 1987a) — with a detection limit of 0.1 mJy — have produced complete samples containing hundreds of radio sources.

We have re-observed two areas from the LBDS, situated in the constellation Hercules (17^h right ascension, 50° declination), improving the sensitivity limits of these fields by a factor of 3 (5 σ – level = 0.45 mJy). This allows us to study the populations of radio galaxies at the milliJansky level. At these flux densities, the dominant population is that of the blue radio galaxies (Kron *et al.*, 1984). As yet, these blue radio galaxies have not been observed in sufficient quantities to determine their global properties and changes in their distribution with cosmic epoch. Deeper surveys will yield additional information on the nature of these blue radio galaxies.

Re-observing areas observed previously at the same resolution and frequency has several advantages. First of all, it greatly simplifies the selfcalibration and reduction process, because a good description of the stronger sources in the fields is already available. Secondly, the photographic plates for optical identification and photometry are already available as well. Thirdly, a direct comparison of the LBDS- and the current maps, will allow us to test the confidence level of a complete sample, i.e. how is the peak flux cut-off in the sample a sufficient safeguard against contamination by spurious sources. Finally, re-obseration at a different epoch makes it possible to search for variable sources.

These questions will be addressed in this paper. Section 2 describes the observations, both observed in the redundancy mode, and reduction of the maps. In section 3, the complete sample is presented. Section 4 discusses the 1412 MHz source counts obtained from the complete samples. Finally, in section 5 a direct comparison is made between the current survey and the LBDS.

2. Observations and reductions.

2.1 OBSERVATIONS. — Observations were carried out with the WSRT 3 km array of the fields Hercules.1 and Hercules.2, which have been observed previously at 21 cm as part of the LBDS. The observations were centred on $\alpha = 17^h18^m58^s$, $\delta = 49°58'00''$ (Her.1), and $\alpha = 17^h15^m33^s$, $\delta = 50°17'00''$ (Her.2) (equinox : 1950).

Both fields were observed with the WSRT Digital Continuum Backend (DCB), using parallel dipoles in the fixed and moveable telescopes. The data were recorded in the redundancy mode, i.e. in addition to the 40 standard interferometers, many interferometers with the same baseline length were included as well.

The observations of Hercules.1 consisted of four 12^h full synthesis measurements in October-November 1983, each with a different shortest spacing (36, 54, 72 and 90 m). Because the DCB was still in its initial stages of implementation, only two of the eight 5 MHz channels were available, centred on 1409.5 and 1414.5 MHz. The effective frequency after combination of the channels is 1412 MHz.

The observations of Hercules.2 consisted of just one 12^h full synthesis (shortest spacing 72 m) in January 1985, but here the full 40 MHz bandwidth (8 channels, each 5 MHz wide) of the DCB could be used, resulting in the same theoretical value for the noise as that of Hercules.1. The effective frequency after combination of the channels is 1402 MHz.

2.2 QUALITY OF THE DATA. — The overall quality of both the Hercules.1 and Hercules.2 measurements was less than average for the WSRT. One 12^h period (the 90 m shortest spacing) of the Hercules.1 measurements had to be discarded completely due to very large phase offsets in the receivers of the moveable telescopes. During the 54 m observation, one of the moveable telescopes was out of order, and the 36 m observation showed frequent periods of outside interference. Only the 72 m observation was completely without problems.

The observations of Hercules.2 had problems with terrestrial interference as well. In addition, the dipoles of one of the moveable telescopes was accidentally rotated by 45 degrees. Although this observation was re-observed in part, a combination with the previous observation did not yield a perfect result.

The details of each observation can be found in table I(a).

For a more detailed discussion of the instrument with respect to deep survey work, see Windhorst *et al.* (1984).

2.3 REDUNDANCY CORRECTIONS. — Because the ten fixed telescopes of the WSRT have an equal separation between the adjacent telescopes (144 m), it is possible to record many interferometers with the same baseline length, but involving different telescopes. This allows one to apply selfcalibration techniques in two stages (see Noordam and de Bruyn, 1982).

The first stage involves correcting for telescope-based errors for each of the time resolution scans (10 s sets of interferometer signals integrated to two-minute scans) which comprise an observation. It is assumed that differences actually observed between the visibilities of all the fixed-fixed telescope interferometers with the same baseline length are caused by telescope-based errors. There are then enough independent equations to yield last-squares solutions of the gain- and phase-errors. These solutions are then used to correct all the raw visibilities.

The second stage involves aligning all the interferometer outputs to the same (relative) phase and flux scale. Time dependent changes in the scales are produced by fluctuations in the ionosphere. For this procedure, it is necessary to use an approximate model of the sky.

The redundancy selfcalibration technique can, in principle, produce a dynamic range of a map to 50000 : 1 or more. However, in practice the dynamic range obtainable in an observation is very dependent on the conditions in the map. Redundancy works best when the signal in each 2 min scan is dominated by a strong point source, preferably at or close to the map center. Extended sources far from the center tend to make the convergence of the iterative alignment procedure toward a correct model of the field more complicated (specifically, a higher time resolution is needed). Both the Hercules fields, for which the map centers were chosen to coincide with the earlier LBDS observations, have a less than ideal configuration of the sources in the map for good redundancy solutions. There are no strong sources close to the field center, and a number of extended sources far from the field center.

Finally, the strongest unresolved source in each map — for which an accurate position was known from high resolution (A-array) VLA maps (Oort *et al.*, 1987) — was used to set the absolute flux scale and position frame.

The redundancy corrections for telescope errors were determined separately for each frequency channel and polarization. A first model for the alignment corrections was determined by updating input positions and fluxes of the 20 brightest sources in the map. The resulting map was cleaned, and the clean components were added to the model. This model was run through the align process several times, until the changes in position of the brightest sources after the update of the model were less than a few tenths of an arcsecond. This final model was used to force each two minute scans to the same gain level and phase.

After application of the redundancy corrections to the raw UV-data, the observations were reprocessed for further reduction.

2.4 DATA REDUCTION. — Because the reduction of the two fields was done in a different manner, the map making procedures are discussed separately.

The observations of the Hercules.1 field were brought to equinox 1950 prior to the Fourier transform. The frequency channels for each 12^h period were Fourier

transformed with the spectral line transform routine LINEMAP (Harten, 1980), using the WSRT Fast Fourier Transform (Brouw, 1971).

The maps of each frequency channel were then combined with weights proportional to the inverse square of the noise of the map. The three maps, each with a different shortest spacing, were combined afterwards in the same manner. Because of the fact that only three of the 4×12^h observations could be used, not all baselines with an 18 m increment were available. The remaining grating rings were removed *via* a cleaning algorithm in the central 1.50×1.94 degrees (Hogbom, 1974). The strongest unresolved sources were subtracted directly from the data before the generation of the maps, and restored after the CLEAN phase.

The same procedure was used to construct a low resolution map. This map was made by excluding the interferometers containing the two outermost telescopes (C & D). This map was used to detect large, diffuse sources that were below the completeness limit in the 3 km map, as well as bridges and halos.

The final high resolution (« 3 km ») map has an overall noise of 80 μJy and a Half Power Beam Width (HPBW) of $12''.0 \times 15''.7$.

The map of Hercules.2 was reduced entirely within the redundancy package. In contrast to the map of Hercules.1, the UV data were not brought to equinox 1950. Grating rings were removed using a Clark-type cleaning algorithm (Clark, 1980). The components in the model used in the aligning phase were subtracted beforehand directly from the data, and restored after cleaning. The final map has an overall noise of 88 μJy and a HPBW of $14''.1 \times 18''.3$. The inner $1^\circ \times 1^\circ$ areas of both maps are shown in figures 1 and 2.

One important first step in the analysis of the maps is the determination of the noise. A radial distance (r) dependent relation of the noise was calculated by studying the distribution of intensities in concentric rings around the field center, using a routine provided by Spoelstra (1980) :

$$\sigma(r) = 85.8 + 39.3\,(r/\mathrm{deg}) - 136.0\,r^2[\mu\mathrm{Jy}]\,(\mathrm{Her.1}),\quad \text{and}$$

$$\sigma(r) = 99.0 - 17.2\,(r/\mathrm{deg}) - 34.6\,r^2[\mu\mathrm{Jy}]\,(\mathrm{Her.2})\,.$$

In order to check that after selfcalibration no systematic offset in the absolute flux level remains, a comparison was made with the sources from the LBDS complete sample. The average difference in flux amounts to less than 1 %, well within the normal uncertainty in the absolute flux calibration at the WSRT.

A similar procedure was used to check for differences in the position frame. In this case, we compared the positions of sources in the current sample with the position of their optical identifications from Windhorst *et al.* (1986). No systematic differences amounting to more than a few tenths of an arcsecond were found.

3. The radio sample.

In this section we will summarize how the source list was obtained for the complete sample of radio sources. Selection criteria and the derivation of intrinsic parameters from the observations will be discussed.

3.1 SOURCE SELECTION AND SOURCE PARAMETERS. — In both the 3 km and low resolution 1.5 km maps, candidate source components were found using the Westerbork point source fitting routine (van Someren-Greve, 1974 ; Brouw and Hoekema, 1970). A cut-off of 4 σ was taken for the peak flux. For the unresolved, resolved and slightly extended sources in this first selection, the observed parameters were determined with a two-dimensional elliptical Gaussian fitting routine (Brinks, 1980). In the case of Hercules.2, the positions of the sources were then precessed to equinox 1950. Master source lists were obtained by selecting only those sources which have $S^p \geqq 5\,\sigma$, where S^p is the peak flux density in the map. The observed source parameters (S^p, position, Gaussian major and minor axis, and the position angle of the major axis from North through East) were determined by fitting the synthesised antenna pattern. A correction for noise induced overestimation of the total flux was applied as well. This correction was determined empirically with Monte-Carlo simulations by Windhorst *et al.* (1984) for 21 cm WSRT observations. The nature of this correction is such that it is reliable and unbiassed only in a statistical sense.

The intrinsic source parameters are those that describe a source as it appears in the sky. The relevant source parameters are the total flux density S^{tot}, the largest angular size (full width at half maximum) ψ and its position angle ϕ. Adopting the unequal double model for each resolved source yields an extra parameter, f, defined as the fractional flux density in the strongest component.

3.2 SAMPLE COMPLETENESS. — Before we proceed to define a complete radio sample, we will first discuss sample completeness in general.

Due to the increasing primary beam attenuation with increasing distance from the field center, it is only possible (without giving up most of the sources in the map) to define a sample which is complete in attenuated peak flux in the map. Therefore, a sample will be complete only for a certain range in S^{tot}, ψ, and f. As a result, a source with a total flux density close to 5 σ is only included in the complete sample if it is close to the field center, and if it is at most marginally resolved. This introduces an incompleteness, which is corrected for by assigning a weight to each source in the master source

list. This weight represents the number of sources with the same total flux, which were not detected or not included in the source list due to the selection criteria.

The correction for the fact that the sample is complete only in terms of map flux is made by giving each source a weight which is inversely proportional to the area over which it would still be included in the complete sample.

It is not necessary to statistically correct for a second cause of incompleteness, the resolution bias. Extended sources of a certain total map flux will drop below the peak flux cut-off more rapidly than an unresolved source of the same total flux. The completeness of a sample therefore depends on angular size and component flux ratio as well. By including the sources found in the low resolution map with $S^{\rm p} > 5\ \sigma$ (low res.), it is possible to increase the completeness of the sample. Any remaining incompleteness due to the resolution bias will be small enough to be ignored (Oort ; 1987a), because at sub-milliJansky flux levels, the bulk of the sources is smaller than 5″ (Oort *et al.*, 1987).

3.3 THE SOURCE LIST. — The complete source lists of both Hercules fields are given in table II. They contain 69 (Her.1) and 71 (Her.2) sources with $S^{\rm p} \geqq 5\ \sigma$. Some of these sources (denoted by an asterisk in the notes) are not included in the complete sample, because they do not satisfy the added criterion that sources in the sample must have a distance to the field center less than 0.464°, or, equivalently, the attenuation factor $ATT < 5$. Sources with an angular separation less than 50″ are considered to be components of one extended source if a bridge or halo is detected. An exception is made for sources with a total flux density $S^{\rm tot} > 10$ mJy. In this case, resolved sources with $\psi^{\rm EQ} < 50''$ (defined as $\psi^{\rm EQ} = \sqrt{1 - \cos^2(\phi)\cos^2(\delta)}$), or components with an angular separation $\psi < 50''$ will be considered to be one extended source, irrespective of the presence of a halo or bridge. An exception is made for source components, which have individually been identified optically.

Table II is organized as follows : All parameters have their 1 σ error estimates listed directly below them. Uncertainties in position and flux were calculated with the quadratic relations :

$$\sigma_\alpha = \sqrt{C_{\rm p}^2 (NR/S^{\rm p})^2 + C_\alpha^2},$$
$$\sigma_\delta = \sqrt{C_{\rm p}^2 (NR/S^{\rm p} \sin\delta)^2 + C_\delta^2}, \quad \text{and}$$
$$\sigma_S = S^{\rm tot} \sqrt{(N/S^{\rm p})^2 + C_S^2 + (\Delta\rho\ \Delta\tau)^2},$$

where N is the (distance dependent) noise, R the normalized source area, $\Delta\rho$ the average pointing error of the individual dishes, and $\Delta\tau = {\rm d}ATT(r)/{\rm d}r$. The value of the constants C_α, C_δ, C_S and $\Delta\rho$ have been determined empirically by Oort and Windhorst (1985) : $C_{\rm p} = 5''.8$, $C_\alpha = 0''.46$, $C_\delta = 0''.41$, $C_S = 0.03$, and $\Delta\rho = 0°.006$.

Column 1 : The source name following the Westerbork convention. The Westerbork survey number (66 W for Her.1, 67 W for Her.2), followed by a sequence number in order of increasing right ascension. Multi-component sources are designated by an asterisk following the source name. Each component is listed directly below, labeled A and B, again in order of right ascension.

Columns 2 and 3 : The right ascension and declination of the source for equinox 1950.

Column 4 : The total flux density, corrected for primary beam attenuation and noise induced flux overestimation.

Column 5 : Resolution code. U = unresolved, R = resolved, E = extended. For a definition of the resolution criteria, see Oort (1987).

Columns 6-9 are given for resolved and extended sources only.

Column 6 : The largest angular size ψ [arcsec]. For resolved sources the deconvolved full width at half maximum. For extended sources, the distance between the two components.

Column 7 : The position angle ϕ [degrees] of the major axis from North through East.

Column 8 : The largest angular size, χ [arcsec], in the direction perpendicular to the major axis ψ.

Column 9 : The component flux ratio *f*.

Column 10 : The sky flux, not corrected for noise overestimation.

Column 11 : The peak flux signal-to-noise ratio.

Column 12 : The normalized source area *R*.

Column 13 : The attenuation factor at the position of the source. Below it, the weight of the source in the source counts.

Column 14 : Notes.

* : The source is not part of the radio complete sample.

@ : The source was below the 5 σ peak flux cut-off in the « 3 km » map, but above the cut-off in the « 1.5 » km map.

V : The source is variable, because the flux found differs by more than 2.5 times the combined flux error from the LBDS flux.

H : A low surface-brightness halo is present.

O : The source was detected in both the Her.1 and Her.2 map.

Column 15 : The alternative name, if the source has been included in a previous catalogue :

53Wxxx : LBDS, Windhorst *et al.* (1984).

OTxxxx : Ohio survey, Brundage *et al.* (1971).

4. The source counts.

The two complete samples were used to construct the 21 cm source counts down to 0.45 mJy. In total,

116 sources were used to determine the counts, of which 4 sources were both with the Hercules.1 and Hercules.2 completeness area. Each source was counted according to its weight, representing the total number of sources expected for a uniform sensitivity over the entire survey area. The weights of the sources in the overlapping area of the two fields were multiplied by 0.52 (to correct for the overlapping area) and counted in each field. The low boundary of the first flux bin was chosen somewhat higher than the 5 σ level of the Hercules.2 field (which has the highest noise of the two fields), to avoid including too many sources with high weights. Each subsequent flux boundary is a factor of two higher than the previous value. The 5 σ differential source counts are given in table III. They are normalized to a Euclidean count of $225 * S^{-5/2}$(/ster/Jy). The 1-σ error bars are determined from the dispersion of the weights in each bin.

Because at the 5 σ level, the contamination of spurious sources may be non-negligible, we have recalculated the source counts, applying a higher peak flux cut-off (7.5 σ). These normalized differential counts are given in table IV. The lowest flux boundary is 0.675 mJy, 1.5 times as high as the lowest flux in the 5 σ counts. They agree with the 5 σ counts to within the uncertainties.

The differential counts are plotted in figure 3, together with the « amalgamated » source counts (Katgert *et al.*, 1987), which were constructed from all WSRT 21 cm surveys available in the literature, including the samples presented here and a number of surveys with a lower noise than the current sample. Our results are in full agreement with these amalgamated counts.

As it is discussed extensively in the paper by Katgert *et al.* (1987), the assumption that the correction for resolution bias is small for sources with flux densities lower than 10 mJy causes severe effects on the value of the source counts close to the 5 σ level of a sample. It is therefore not surprising that when the source counts from the current sample are compared with the values found from the LBDS (Windhorst *et al.*, 1984) — where a correction for resolution bias was applied with the assumption that the median angular size of radio sources at the milliJansky level is $\sim 7''$ —, differences amounting to a factor of two or more are seen. This is an indirect indication that our assumption about the resolution correction is correct. At the LBDS flux levels, the corrections for resolution bias for the current survey are small regardless of the exact distribution of angular sizes of mJy sources, because the noise level is a factor of two or more lower than in the LBDS maps. Disregarding the resolution corrections in the LBDS brings the value of the source counts to better agreement with the current survey. This has been confirmed by other WSRT deep surveys as well (see e.g. Oort, 1987a).

The apparent lack of radio sources with flux densities of ~ 1 mJy with respect to a smooth interpolation of the source counts above and below 1 mJy, which is seen in other deep surveys (Oort, 1987a ; Mitchell and Condon, 1985), is present in the Hercules fields as well. This indicates that this small scale structure in the source counts may not be a local fluctuation, particular to an individual field, but may be a general property of the source counts. An explanation of the cause of this structure may be that the Radio Luminosity Function of blue radio galaxies has a very sharp cut-off at high radio powers.

5. A direct comparison with the LBDS Hercules fields.

The fact that the very same fields discussed here were observed previously at 21 cm with the WSRT as part of the LBDS (Windhorst *et al.*, 1984), gives us an ideal opportunity to check the consistency of results obtained from complete samples from the same area in the sky, but with different signal-to-noise ratios. In particular, we will address the question whether the 5 σ peak flux cut-off for inclusion of a source in the complete sample is sufficient to ensure minimal contamination by spurious sources.

The maps of the LBDS survey of Hercules.1 and Hercules.2 were made with one 12^h continuum observation with a total bandwidth of 10 MHz. The size of the beam in each map is equal to that of the Hercules.1 beam in the current survey. The noise in the maps is, however, a factor of 3 higher than in the current survey (~ 0.22 mJy). The large similarities between the two surveys make a comparison straightforward. Moreover, because the LBDS maps were made in 1980, it will be possible to find variable sources in the maps as well.

5.1 SPURIOUS SOURCES IN THE LBDS. — In addition to a comparison between the sources found in the LBDS and the current survey, one can also investigate the sources in the LBDS complete sample and the additional source list which should have been found, but were *not* found in the current survey. Sources with a peak flux between 5 and 6 σ are counted with large weights in the source counts, because they are assumed to represent a large number of counterparts with equal flux density, not included in the complete sample due to the non-uniformity of the sensitivity over the survey area. Thus, a few spurious sources near the flux limit may cause a significant overestimation of the source counts.

If the noise in a radio map is purely random, the number of noise pixels above a certain signal-to-noise level decreases rapidly when this level is increased. Above 4 σ, the number of spurious peaks within the maximum attenuation radius of the map, which would be included in the sample is theoretically 10. At 5 σ, the number falls below unity (~ 0.2), which is why this cut-off level has been used for most WSRT deep surveys.

In practice, however, the noise in the map does have structure. Consider, for instance, the fact that the noise level changes with distance to the field center. The proximity of strong sources or remnants of their grating rings may cause additional local variations in the noise level.

The factor of three differences between the noise level of the LBDS and the current survey gives us an opportunity to measure the contamination in practice. The results of this comparison are given in table V, along with a similar comparison made for the LBDS map of Lynx.2 and the deeper map made by Oort and Windhorst (1985), and the overlapping area of the LBDS-Lynx.3 and the deeper Lynx.3A (Oort, 1987a) field.

As it was to be expected, the fraction of spurious sources between 4 and 5 σ (LBDS) is large. Over two thirds of the LBDS suspected detections at these signal-to-noise levels are not found in the current maps. More surprising is the fact, that even above 5 $\sigma_{\rm LBDS}$ five sources are not seen in our maps, one of which has a solid identification with a 20$^{\rm th}$ magnitude elliptical galaxy : they are 53W006, 53W011, 53W013, 53W025, and 53W032. Variability cannot explain the disappearance of these sources, because that would mean a reduction of more than a factor of four in flux, which is very unlikely. Moreover, VLA high resolution observations of two of these sources at a different epoch showed no detection.

The large fraction of spurious sources (5 out of 15) in the Hercules fields may be largely due to the fact that there is a large number of strong ($>$ 100 mJy) sources present in the field. For instance, the spurious source 53W011 results from a superposition of remnants of the grating rings of the sources 53W008 and 53W031. The other two fields, Lynx.2 and Lynx.3A, have no sources stronger than 50 mJy in the overlapping area, and show less contamination by spurious sources (3 out of 22). Even so, the number of spurious sources even in these fields is too large for comfort.

We must conclude that only a 6 σ peak flux cut-off — where no spurious sources are found — ensures that no spurious sources are present in a complete sample. This is especially true for areas in the sky where strong radio sources are present.

In the current sample we have used a different approach to limit as much as possible the contamination by spurious sources. Each individual source with a peak flux between 5 and 6 σ was inspected in detail before inclusion in the complete sample. The shape of the source and the irregularity of the local background were taken into consideration. We are confident that the contamination still present in the current complete sample is small.

5.2 VARIABLE SOURCES. — The different epochs of the LBDS maps of Hercules (1980.52) and the current observations of Hercules.1 (1983.83) and Hercules.2 (1985.04) makes it possible to search for sources which are variable on time scales of a few years. A source is designated as a variable when its flux in the current survey differs from the LBDS flux by more than 2.5 times the combined flux error. Six sources meet this requirement : 66W012, 66W022, 66W051, 66W060, 67W014, and 67W053. Three sources have also been observed at high resolution at an intermediate epoch (Oort *et al.*, 1987). The flux at each epoch is given in table VI. We list some of their particulars here :

66W012 = 53W054A : This radio source was listed as a component of an extended source in the LBDS, but each component has since then been individually optically identified (Windhorst *et al.*, 1986). This component is associated with a blue galaxy.

66W022 = 53W062 : This source is associated with a blue galaxy (Windhorst *et al.*, 1984b). It is unresolved in the VLA high resolution map ($\psi < 1''$).

66W051 = 53W078 : This source is associated with a red galaxy (Windhorst *et al.*, 1984b). The radio extent from the VLA map is 4.5″. It has steadily decreased in flux through the years.

66W060 = 53W084 : This source is not included in the LBDS radio complete sample. It has not been optically identified.

67W014 = 53W014 : This source is associated with a quasar (Windhorst *et al.*, 1986). The radio extent from the VLA map is 3″.

67W053 = 53W045 : This source is associated with a red galaxy (Windhorst *et al.*, 1986). It is unresolved by the WSRT beam and has decreased in flux by almost a factor of four in 3 1/2 years.

Variability on time scales of $\sim$ 1 year is not uncommon in quasars. Blue radio galaxies which only exhibit an unresolved ($\psi < 1''$) core frequently show a similar behaviour (Oort, 1987b), indicating that the radio emission is coming from a region only a few parsecs in diameter. It is not clear why the two radio sources associated with red radio galaxies, which usually show extended emission, should steadily decrease in flux. It may be that these radio galaxies have a variable compact core as well.

6. Conclusions.

(1) The small scale structure in the source counts at $\sim$ 1 mJy, found in previous surveys (Oort, 1987a), is also visible in the current survey. Because this increases the area in the sky where this structure is observed, it becomes more probable that it is a general property of the source counts.

(2) A comparison between the current survey and the observations of the same area in the LBDS (Windhorst *et al.*, 1984) shows that the 5 σ peak flux cut-off in the complete sample is not sufficient to exclude contamina-

tion by spurious sources. This contamination is especially severe when strong sources are present in the field.

(3) Six sources are found which are either variable on time scales of a year, or steadily decrease in flux with time. Two of these variable sources are associated with blue radio galaxies, which frequently seem to exhibit this property. It indicates that the radio emission is emitted from a small non-thermal nucleus.

Acknowledgements.

We would like to thank Ger de Bruyn and Wim Brouw for their help and valuable advice concerning the redundancy techniques. Peter Katgert looked over our shoulder from time to time and with his expertise contributed to solving some of the problems with the reduction and analysis.

The Leiden computer group was very helpful with the reduction on the IBM. Loek Zuyderduin is thanked for photographing the tables in this paper, and Christine Oort for doing part of the typing.

MJAO acknowledges ASTRON/ZWO for financial support (grant 782-373-009).

The Westerbork Radio Observatory is operated by the Netherlands Foundation for Radio astronomy with the financial support of the Netherlands Organisation for the Advancement of Pure Research (ZWO).

References

BRINKS, E. : 1980, private communication.
BROUW, W. N. : 1971, Ph. D. Thesis, University of Leiden.
BROUW, W. N., HOEKEMA, T. : 1970, Internal Technical Report of the Netherlands Foundation for Radio astronomy (NFR) 87.
BRUNDAGE, R. K., DIXON, R. S., EHMAN, J. R., KRAUS, J. D. : 1971, *Astron. J.* **76,** 777.
CLARK, B. G. : 1980, *Astron. Astrophys.* **89,** 377.
HÖGBOM, J. A. : 1974, *Astron. Astrophys. Suppl. Ser.* **15,** 417.
HARTEN, R. H. : 1979, Internal Technical report of the NFR 151.
KATGERT, P., OORT, M. J. A., WINDHORST, R. A. : 1987, *Astron. Astrophys. Lett.* (submitted).
KATGERT-MERKELIJN, J. K., ROBERTSON, J. G., WINDHORST, R. A., KATGERT, P. : 1985, *Astron. Astrophys. Suppl. Ser.* **61,** 517.
NOORDAM, J. E., DE BRUYN, A. G. : 1982, *Nature* **299,** 597.
OORT, M. J. A. : 1987a, *Astron. Astrophys. Suppl.* (in press).
OORT, M. J. A. : 1987b, Thesis University of Leiden.
OORT, M. J. A., KATGERT, P., STEEMAN, F. W. M., WINDHORST, R. A. : 1987, *Astron. Astrophys.* **179,** 41.
OORT, M. J. A., WINDHORST, R. A. : 1985, *Astron. Astrophys.* **145,** 405.
VAN SOMEREN-GREVE, H. W. : 1974, *Astron. Astrophys. Suppl. Ser.* **15,** 343.
SPOELSTRA, T. A. Th. : 1980, Internal Technical Report of the NFR 60.
WINDHORST, R. A., VAN HEERDE, G. M., KATGERT, P. : 1984, *Astron. Astrophys. Suppl. Ser.* **58,** 1.
WINDHORST, R. A., KRON, R. G., KOO, D. C. : 1984b, *Astron. Astrophys. Suppl. Ser.* **58,** 39.
WINDHORST, R. A., DRESSLER, A., KOO, D. C. : 1986, *IAU Symposium 124 « Observational Cosmology »* G. Burbidge and L. Z. Fang (Eds) (Reidel, Dordrecht) p. 573.

TABLE I. — *The characteristics of the WSRT observations.*

spacing m	epoch YY.DDD	noise μJy	field
36	83.223	132	Hercules.1
54	83.244	142	Hercules.1
72	83.313	98	Hercules.1
combined	83.260	80	Hercules.1
72	85.014	83	Hercules.2

TABLE II. — *The source list for complete sample.*

NAME	RA(1950.0) H M S	DEC(1950.0) O ' ''	S1412 (mJy)	RES	PSI ('')	FI (O)	CHI ('')	F	SSKY (mJy)	SP/N	R	ATTEN WEIGHT	NOTES	OTHER NAMES
66W001	17 16 3.31 0.06	49 52 25.7 0.7	9.24 0.72	R	6.4 3.9	76 15	5.3	0.50	9.24 0.72	18.49	1.23	5.552 * 0.000		53W041
66W002	17 16 7.98 0.07	49 51 34.2 0.7	5.56 0.50	U					5.56 0.50	14.21	1.02	5.168 * 0.000		53W042
66W003	17 16 17.51 0.19	49 46 26.8 2.3	2.51 0.52	R	15.4 4.9	137 11	0.0	0.73	2.92 0.61	5.03	1.48	5.309 * 0.000		
66W004	17 16 21.53 0.12	50 6 11.7 1.5	2.05 0.34	U					2.34 0.39	6.37	1.15	4.197 1.000		53W044
66W005	17 16 38.19 0.05	50 10 56.2 0.4	62.0 3.2	R	3.3 0.6	112 22	0.0	0.50	62.0 3.2	197.53	1.03	3.944 1.000		53W046
66W006	17 16 53.52 0.06	50 25 48.6 0.5	21.9 1.8	R	6.0 3.5	42 22	2.2	0.75	21.9 1.8	24.58	1.08	12.945 * 0.000		53W047
66W007	17 17 6.76 0.09	49 32 47.7 1.1	3.58 0.52	U					3.68 0.53	7.61	0.91	7.654 * 0.000		
66W008	17 17 14.22 0.05	49 51 36.0 0.4	131.3 5.3	R	20.4 2.0	25 21	4.1	0.60	131.3 5.3	367.45	2.24	1.874 1.000		53W051
66W009	17 17 17.46 0.11	49 58 59.7 1.2	1.84 0.21	R	9.4 5.3	41 6	0.0	0.50	1.87 0.21	9.28	1.40	1.668 1.383		
66W010	17 17 17.50 0.13	49 51 55.9 1.5	0.79 0.15	U					0.82 0.16	5.36	1.00	1.794 2.324		
66W011	17 17 18.72 0.05	50 1 56.1 0.4	8.00 0.34	U					8.00 0.34	54.63	1.00	1.694 1.000		53W052
66W012	17 17 31.22 0.08	49 48 51.9 0.8	2.07 0.19						2.07 0.19	12.20	1.14	1.724 1.108	V	53W054A
66W013	17 17 33.85 0.08	49 49 15.1 0.9	2.08 0.19						2.08 0.19	11.86	1.22	1.661 1.157		53W054B
66W014	17 17 36.33 0.80	49 55 49.9 10.1	3.34 0.51	R	37.9 10.1	92 5	38.7	0.50	5.55 0.85	6.74	4.70	1.409 2.371	a	
66W015	17 17 50.83 0.13	50 10 42.1 1.6	0.54 0.11	U					0.56 0.11	5.10	0.74	1.719 2.683		
66W016	17 17 51.31 0.06	49 48 45.5 0.6	1.96 0.14	U					1.96 0.14	16.12	0.94	1.475 1.029		53W057
66W017	17 18 3.49 0.14	50 0 42.5 1.7	1.25 0.17	R	15.4 5.3	59 7	0.0	0.70	1.30 0.18	7.63	1.64	1.174 2.597		53W058
66W018	17 18 5.05 0.05	50 3 20.7 0.4	19.4 1.0	R	5.0 0.8	59 8	0.0	0.69	19.4 1.0	172.18	1.06	1.213 1.000		53W059
66W019	17 18 8.34 0.06	49 31 44.1 0.6	7.18 0.53	U					7.18 0.53	19.48	1.03	4.757 1.000		53W060
66W020	17 18 8.88 0.13	50 15 29.4 1.5	0.90 0.17	U					0.96 0.18	5.35	1.03	2.067 1.927		
66W021	17 18 11.26 0.07	49 47 1.1 0.7	4.76 0.43	E	24.5 3.0	57 20	0.0	0.50	4.76 0.44	12.52	0.79	1.408 1.253	H	53W061
66W022	17 18 16.68 0.10	50 2 6.7 1.1	0.73 0.10	U					0.76 0.10	7.53	1.02	1.123 2.873	V	53W062
66W023	17 18 22.87 0.10	50 1 23.2 1.2	0.39 0.06	U					0.40 0.06	6.91	0.60	1.086 3.692		
66W024	17 18 24.64 0.05	50 0 37.5 0.4	5.54 0.20	U					5.54 0.20	57.55	1.02	1.070 1.000		53W065
66W025	17 18 27.68 0.05	50 4 2.1 0.4	4.27 0.17	U					4.27 0.17	43.25	0.99	1.122 1.000		53W066
66W026	17 18 36.58 0.05	50 13 54.0 0.4	21.9 0.9	R	8.9 1.2	99 10	4.8	0.50	21.9 0.9	109.64	1.38	1.676 1.000		53W067
66W027	17 18 36.71 0.15	50 5 11.5 1.8	0.57 0.11	U					0.67 0.13	5.37	1.25	1.129 7.666		
66W028	17 18 43.32 0.06	49 39 6.8 0.6	3.09 0.20	U					3.09 0.20	19.55	0.92	2.043 1.000		53W068
66W029	17 18 43.62 0.14	49 46 35.9 1.6	0.59 0.11	U					0.66 0.13	5.31	1.09	1.297 4.691		
66W030	17 18 46.53 0.05	49 47 48.0 0.5	3.82 0.17	R	5.0 2.8	65 26	3.7	0.50	3.82 0.17	31.77	1.10	1.229 1.000		53W069
66W031	17 18 51.12 0.17	49 46 48.1 2.1	0.76 0.14	U					0.87 0.16	5.37	1.43	1.275 4.771		
66W032	17 18 51.12 0.06	50 8 57.6 0.5	2.56 0.14	U					2.56 0.14	23.92	0.96	1.262 1.000		53W070
66W033	17 18 51.87 0.09	50 24 46.8 1.0	3.60 0.43	U					3.68 0.43	9.54	1.16	4.385 1.000		
66W034	17 18 56.81 0.06	50 20 12.3 0.6	4.24 0.29	U					4.24 0.29	19.91	0.97	2.684 1.000		53W071
66W035	17 18 57.09 0.10	50 0 4.9 1.1	0.63 0.09	U					0.65 0.09	7.49	0.99	1.008 3.645		
66W036	17 19 5.73 0.12	49 49 55.6 1.5	0.78 0.11	U					0.86 0.13	6.94	1.24	1.136 3.325		

TABLE II *(continued)*.

NAME	RA(1950.0) H M S	DEC(1950.0) O ' ''	S1412 (mJy)	RES	PSI ('')	FI (O)	CHI ('')	F	SSKY (mJy)	SP/N	R	ATTEN WEIGHT	NOTES	OTHER NAMES
66W037	17 19 8.92 0.11	49 53 52.9 1.4	0.36 0.06	U					0.38 0.06	6.00	0.69	1.039 6.778		
66W038	17 19 15.30 0.07	50 25 29.6 0.7	5.71 0.49	U					5.71 0.49	15.00	1.05	4.859 1.003		53W072
66W039	17 19 19.83 0.19	50 2 43.7 2.3	1.01 0.16	R	13.5 5.3	37 31	6.4	0.60	1.09 0.18	6.23	1.85	1.068 5.227		
66W040	17 19 26.34 0.05	49 46 42.5 0.4	96.8 3.3	U					96.8 3.3	825.78	1.00	1.331 1.000		53W075
66W041	17 19 34.95 0.13	49 42 30.2 1.6	0.65 0.13	U					0.67 0.13	5.20	0.88	1.713 2.641		
66W042	17 19 36.61 0.15	49 45 45.4 1.8	0.78 0.14	U					0.90 0.16	5.58	1.28	1.440 3.206		
66W043	17 19 38.76 0.17	50 19 32.0 2.1	1.82 0.33	R	14.2 4.9	135 45	0.0	0.50	1.98 0.36	5.74	1.53	2.761 1.356		
66W044	17 19 39.74 0.07	49 42 56.1 0.8	1.94 0.17	U					1.94 0.17	12.40	1.07	1.701 1.004		53W076
66W045	17 19 44.28 0.11	49 51 24.0 1.3	6.51 0.39	R	17.5 3.0	82 9	2.6	0.50	6.93 0.41	20.28	3.19	1.209 1.012		53W077
66W046	17 19 48.91 0.34	49 43 33.7 4.3	1.68 0.31	U					1.91 0.35	5.53	1.63	1.714 2.396	a	
66W047	17 19 50.05 0.12	49 59 47.7 1.4	0.60 0.10	U					0.63 0.11	6.07	1.02	1.150 4.507		
66W048	17 19 53.09 0.13	50 18 09.9 1.5	0.77 0.15	U					0.81 0.16	5.19	0.72	2.636 1.542		
66W049	17 19 56.82 0.25	50 1 38.2 3.1	1.64 0.27	R	18.3 5.4	32 5	0.0	0.50	1.59 0.27	6.07	2.44	1.217 3.862		
66W050	17 19 57.05 0.15	50 1 41.4 1.8	1.18 0.17	R	11.5 5.4	33 8	0.0	0.50	1.25 0.18	7.24	1.60	1.220 2.675		
66W051	17 20 3.09 0.11	50 6 26.1 1.3	0.74 0.12	U					0.76 0.12	6.54	0.93	1.417 2.469	V	53W078
66W052	17 20 3.66 0.49	50 10 35.3 6.1	2.64 0.48	R	25.0 9.9	130 41	27.4	0.50	2.84 0.51	5.67	2.40	1.692 2.340	a	
66W053	17 20 4.33 0.14	49 30 48.5 1.7	6.36 0.83	R	14.1 5.3	144 23	5.0	0.62	6.49 0.85	8.40	1.78	5.987 0.000	*	
66W054	17 20 7.98 0.05	50 13 21.3 0.4	11.7 0.5	R	6.3 1.7	9 10	0.0	0.59	11.7 0.5	63.84	1.07	2.041 1.000		53W079
66W055	17 20 22.07 0.05	49 58 31.2 0.4	25.9 0.9	R	10.8 1.2	31 24	2.8	0.70	25.9 0.9	165.17	1.26	1.424 1.000		53W080
66W056	17 20 22.55 0.05	50 0 47.8 0.4	12.1 0.5	U					12.1 0.5	94.39	1.01	1.451 1.000		53W081
66W057	17 20 22.82 0.06	50 11 17.3 0.6	2.50 0.19	U					2.50 0.19	15.38	0.94	2.041 1.000		53W082
66W058	17 20 32.48 0.07	49 49 55.2 0.7	1.89 0.16	U					1.89 0.16	13.28	0.93	1.787 1.032		
66W059	17 20 33.84 0.05	50 5 29.0 0.5	5.01 0.25	U					5.01 0.25	32.00	1.03	1.774 1.000		53W083
66W060	17 20 34.74 0.11	49 51 19.4 1.4	0.68 0.12	U					0.71 0.12	6.00	0.78	1.753 2.070	V	53W084
66W061	17 20 37.03 0.05	49 57 23.6 0.5	4.52 0.22	U					4.52 0.22	31.03	1.03	1.640 1.000		53W085
66W062	17 20 41.59 0.09	49 56 24.6 1.0	4.06 0.30	R	16.0 4.4	109 5	0.0	0.69	4.06 0.30	15.60	1.75	1.729 1.000		53W086
66W063	17 20 44.18 0.05	50 14 41.2 0.4	14.1 0.7	U					14.1 0.7	55.03	1.02	3.153 1.000		53W088
66W064	17 20 44.22 0.06	50 11 30.4 0.6	5.58 0.35	R	6.1 3.5	82 9	2.7	0.52	5.58 0.35	22.37	1.18	2.571 1.000		53W087
66W065	17 20 46.16 0.07	50 9 45.7 0.7	3.04 0.26	U					3.04 0.26	13.88	1.10	2.398 1.000		53W089
66W066	17 21 8.48 0.13	49 59 29.6 1.5	1.19 0.20	U					1.37 0.24	5.98	1.15	2.398 1.479		53W090
66W067	17 21 17.77 0.05	50 8 47.3 0.4	22.6 1.1	U					22.6 1.1	81.33	1.00	3.525 1.000		53W091
66W068	17 21 26.36 0.09	49 50 4.7 1.0	1.75 0.22	U					1.79 0.23	8.44	0.75	3.633 1.000		
66W069	17 21 39.53 0.17	50 16 8.7 2.0	5.65 0.95	R	12.9 5.3	168 13	0.0	0.50	6.09 1.02	6.43	1.63	8.461 0.000	*	

TABLE II *(continued)*.

NAME	RA(1950.0) H M S	DEC(1950.0) O ' ''	S1412 (mJy)	RES	PSI ('')	FI (O)	CHI ('')	F	SSKY (mJy)	SP/N	R	ATTEN WEIGHT	NOTES	OTHER NAMES
67W001	17 12 56.48 0.07	49 56 35.4 0.6	25.2 1.9	R	9.3 3.3	155 19	4.4	0.57	25.2 1.9	26.17	1.28	9.480 0.000	*	53W001
67W002	17 12 59.91 0.06	50 18 51.8 0.4	48.5 2.4	R	9.4 1.2	21 9	2.3	0.54	48.5 2.4	134.46	1.24	3.386 1.000		53W002
67W003	17 13 2.50 0.17	50 21 39.4 2.1	1.42 0.29	U					1.67 0.34	5.09	1.13	3.368 2.282		53W003
67W004	17 13 21.60 0.06	50 13 46.3 0.4	54.3 2.4	R	8.8 1.0	25 17	3.6	0.56	54.3 2.4	205.95	1.21	2.459 1.000		53W004
67W005	17 13 22.60 0.12	50 31 42.9 1.3	6.59 0.63	R	11.8 4.6	69 21	9.3	0.61	6.59 0.63	12.13	1.69	3.754 1.000		53W005
67W006	17 13 32.93 0.15	50 23 14.7 1.8	0.69 0.13	U					0.73 0.14	5.27	0.69	2.236 1.803		
67W007	17 13 48.08 0.06	49 57 36.3 0.4	305.4 15.4	R	8.2 0.8	125 32	5.6	0.50	305.4 15.4	742.26	1.25	3.844 1.000		OT+523.3
67W008	17 13 49.05 0.06	50 24 45.2 0.4	91.0 3.7	R	19.6 2.0	13 7	4.4	0.50	91.0 3.7	236.59	2.20	1.933 1.000		53W009
67W009	17 13 50.32 0.07	50 13 36.9 0.6	7.72 0.39	R	11.4 2.7	101 12	9.1	0.60	7.72 0.39	30.01	1.62	1.731 1.000		53W010
67W010	17 13 53.64 0.06	50 3 46.9 0.5	38.1 1.7	R	18.4 2.0	25 20	7.2	0.62	38.1 1.7	93.33	1.96	2.340 1.000		53W012
67W011	17 13 54.47 0.14	49 59 1.2 1.7	1.69 0.28	U					1.92 0.32	6.25	1.12	3.162 1.153		
67W012	17 14 0.05 0.12	50 9 11.8 1.4	0.72 0.11	U					0.74 0.11	6.74	0.70	1.735 1.820		
67W013	17 14 2.36 0.11	50 0 36.8 1.2	0.99 0.13	U					1.01 0.13	8.26	0.54	2.607 1.095		
67W014	17 14 2.44 0.07	50 3 47.4 0.7	3.03 0.21	U					3.03 0.21	18.02	0.88	2.140 1.000	V	53W014
67W015	17 14 8.71 0.06	50 16 29.0 0.4	180.4 6.4	R	14.9 1.5	139 15	7.6	0.53	180.4 6.4	740.23	1.84	1.420 1.000		53W015
67W016	17 14 9.09 0.15	49 59 23.8 1.8	1.87 0.29	U					2.06 0.32	6.80	1.29	2.671 1.227		53W016
67W017	17 14 21.31 0.07	50 47 28.5 0.6	31.4 2.3	R	11.7 3.1	35 13	0.0	0.50	31.4 2.3	27.69	1.46	9.772 0.000	*	53W017
67W018	17 14 23.58 0.17	50 8 5.5 2.0	0.69 0.13	U					0.79 0.15	5.19	1.11	1.481 3.511		
67W019	17 14 30.10 0.11	49 58 14.1 1.3	1.41 0.19	U					1.44 0.20	7.74	0.85	2.471 1.183		
67W020	17 14 32.75 0.08	50 33 23.0 0.7	5.88 0.36	R	11.6 3.6	24 5	1.1	0.50	5.88 0.36	22.28	1.44	2.036 1.000		53W019
67W021	17 14 34.30 0.06	50 28 15.3 0.5	6.63 0.30	R	9.6 2.6	34 9	0.0	0.50	6.63 0.30	36.67	1.29	1.515 1.000		53W020
67W022	17 14 41.73 0.20	50 21 42.2 2.2	0.87 0.16	U					0.98 0.17	5.71	1.52	1.186 4.933		
67W023	17 14 50.13 0.06	50 23 55.4 0.5	4.07 0.18	R	6.4 2.9	39 12	0.0	0.59	4.07 0.18	31.96	1.11	1.199 1.000		53W021
67W024*	17 14 54.35 0.06	50 27 38.7 0.8	10.1 0.4	E	17.1	67 5	0.0	0.51	10.1 0.4	32.65	2.46	1.338 1.000	C	53W022
A	17 14 53.52 0.07	50 27 35.4 0.6	4.98 0.25						4.98 0.25	27.12	1.46	1.340		
B	17 14 55.17 0.06	50 27 42.1 0.5	5.12 0.22						5.12 0.22	40.67	1.00	1.337		
67W025	17 14 54.97 0.06	50 8 47.3 0.4	114.6 3.8	R	13.8 1.4	59 12	5.9	0.74	114.6 3.8	720.57	1.37	1.222 1.000		53W023
67W026	17 14 55.47 0.06	50 0 0.8 0.5	10.6 0.5	R	6.9 1.9	38 14	3.5	0.60	10.6 0.5	54.04	1.14	1.892 1.000		53W024
67W027	17 14 59.26 0.09	50 36 57.9 0.9	2.07 0.20	U					2.07 0.20	11.67	0.85	2.338 1.000		
67W028	17 15 0.17 0.15	50 2 18.3 1.8	0.49 0.10	U					0.51 0.10	5.26	0.66	1.606 2.893		
67W029	17 15 5.76 0.11	50 21 15.2 1.2	0.62 0.08	U					0.63 0.08	8.03	0.76	1.073 2.786		
67W030*	17 15 11.75 0.09	50 27 7.9 2.0	6.58 0.42	E	29.9	112 5	18.8	0.62	6.58 0.42	15.76	3.53	1.245 1.161	C	53W027
A	17 15 10.19 0.08	50 27 14.0 0.8	2.52 0.17						2.52 0.17	17.15	1.23	1.254		
B	17 15 13.08 0.13	50 27 2.7 1.5	4.05 0.30						4.05 0.30	15.01	2.30	1.237		
67W031	17 15 12.16 0.06	49 50 24.2 0.5	19.0 1.1	R	7.1 2.2	52 14	0.0	0.58	19.0 1.1	44.49	1.15	4.389 1.000		53W026
67W032	17 15 13.47 0.11	50 39 46.3 1.3	2.78 0.33	U					2.86 0.34	9.28	1.22	2.893 1.000		53W028
67W033	17 15 14.66 0.06	50 23 33.8 0.4	23.3 0.7	R	5.0 0.7	25 25	0.0	0.70	23.3 0.7	212.04	1.03	1.103 1.000		53W029
67W034	17 15 21.29 0.09	49 46 46.3 1.0	5.55 0.62	U					5.51 0.61	10.68	0.91	6.942 0.000	*	
67W035	17 15 24.81 0.23	49 57 4.8 2.8	2.74 0.42	R	16.6 5.3	25 26	0.0	0.50	2.77 0.42	6.82	2.06	2.202 1.422		

TABLE II *(continued)*.

NAME	RA(1950.0) H M S	DEC(1950.0) ° ' ''	S1412 (mJy)	RES	PSI ('')	FI (°)	CHI ('')	F	SSKY (mJy)	SP/N	R	ATTEN WEIGHT	NOTES	OTHER NAMES
67W036	17 15 28.01 0.08	50 12 51.4 0.8	1.26 0.11	U					1.26 0.11	12.88	0.97	1.034 1.585		53W030
67W037	17 15 30.66 0.06	49 59 54.7 0.4	118.4 4.6	R	7.1 0.7	85 7	4.8	0.74	118.4 4.6	644.15	1.14	1.771 1.000		53W031
67W038	17 15 31.58 0.10	50 13 9.1 2.2	0.54 0.11	U					0.62 0.12	5.11	1.21	1.029 24.534		
67W039	17 15 37.12 0.06	49 48 29.2 0.5	17.9 1.1	R	7.0 2.7	58 13	0.0	0.58	17.9 1.1	34.06	1.16	5.446 0.000	*	53W033
67W040*	17 15 37.89 0.07	50 3 53.6 1.1	8.67 0.41	E	36.0	38 5	0.0	0.70	8.67 0.41	23.93	2.78	1.395 1.000		53W034
A	17 15 36.88 0.06	50 3 41.3 0.6	6.06 0.28						6.06 0.28	34.23	1.34	1.409		
B	17 15 39.21 0.09	50 4 9.6 1.0	2.58 0.20						2.58 0.20	14.14	1.41	1.377		
67W041	17 15 41.08 0.06	50 21 49.2 0.5	3.68 0.15	U					3.68 0.15	37.33	0.96	1.048 1.000		53W035
67W042	17 15 42.31 0.07	50 32 12.5 0.6	4.18 0.22	U					4.18 0.22	26.91	1.07	1.574 1.000		53W036
67W043	17 15 44.97 0.06	50 22 25.6 0.4	6.76 0.24	R	5.7 1.7	33 34	0.0	0.60	6.76 0.24	61.00	1.07	1.065 1.000		53W037
67W044*	17 15 45.40 0.10	50 46 59.2 1.7	10.6 1.2	E	19.2	144 5	0.0	0.51	10.6 1.2	8.99	2.14	6.714 0.000	*	53W038
A	17 15 44.82 0.10	50 47 7.0 1.0	5.43 0.64						5.43 0.64	9.80	0.99	6.833	*	
B	17 15 45.99 0.12	50 46 51.4 1.3	5.12 0.69						5.12 0.69	8.25	1.15	6.597	*	
67W045	17 15 47.60 0.07	50 28 41.1 0.6	2.98 0.17	U					2.98 0.17	21.12	1.14	1.314 1.000		53W039
67W046	17 15 48.92 0.09	50 40 19.5 1.0	2.12 0.23	U					2.14 0.24	10.09	0.80	3.034 1.000		
67W047	17 16 3.25 0.07	49 52 26.1 0.6	8.69 0.55	R	6.2 3.4	34 34	0.0	0.59	8.69 0.55	25.69	1.10	3.582 1.000	O	53W041
67W048	17 16 8.00 0.07	49 51 33.7 0.7	6.08 0.46	U					6.08 0.46	17.90	1.00	4.015 1.001	O	53W042
67W049	17 16 14.34 0.17	49 58 17.0 2.0	0.97 0.19	U					1.12 0.22	5.16	1.11	2.182 1.895		
67W050	17 16 15.00 0.07	50 21 59.8 0.6	2.44 0.13	U					2.44 0.13	23.61	0.94	1.143 1.000		53W043
67W051	17 16 18.49 0.20	50 4 15.6 2.4	0.85 0.17	U					0.98 0.19	5.18	1.34	1.519 3.323		
67W052	17 16 21.53 0.08	50 6 11.5 0.8	2.17 0.16	U					2.17 0.16	15.16	1.09	1.408 1.015	O	53W044
67W053	17 16 26.61 0.14	50 18 51.7 1.6	0.43 0.07	U					0.44 0.08	5.81	0.69	1.158 5.029	V	53W045
67W054	17 16 32.14 0.14	50 10 24.0 1.6	0.49 0.09	U					0.51 0.09	5.77	0.72	1.291 3.757		
67W055	17 16 38.15 0.06	50 10 56.2 0.4	66.6 2.3	R	6.3 0.7	43 9	2.6	0.61	66.6 2.3	483.16	1.11	1.323 1.000	O	53W046
67W056	17 16 53.40 0.06	50 25 49.3 0.4	24.8 0.9	R	7.0 1.0	36 22	3.5	0.73	24.8 0.9	152.34	1.10	1.602 1.000	O	53W047
67W057	17 16 55.12 0.10	50 20 47.3 1.1	0.80 0.10	U					0.82 0.10	8.85	0.70	1.433 1.662		
67W058	17 16 56.64 0.07	50 27 5.0 0.6	10.9 0.5	R	16.1 2.6	80 12	5.8	0.69	10.9 0.5	40.23	1.72	1.727 1.000		53W048
67W059	17 16 57.15 0.06	50 36 18.6 0.4	104.3 5.0	R	21.0 2.1	67 5	8.6	0.62	104.3 5.0	152.92	2.57	3.046 1.000		53W049
67W060	17 17 14.20 0.06	49 51 36.7 0.5	136.5 8.2	R	20.3 2.1	27 19	7.9	0.60	136.5 8.2	109.62	2.24	6.796 0.000	* O	53W051
67W061	17 17 17.27 0.17	49 58 58.4 2.1	1.90 0.35	U					2.16 0.39	5.71	1.29	3.408 1.166		
67W062	17 17 18.60 0.06	50 1 55.8 0.5	8.08 0.46	R	6.7 3.1	23 23	0.0	0.56	8.08 0.46	30.47	1.08	2.801 1.000	O	53W052
67W063	17 17 34.05 0.10	50 42 54.6 1.1	15.6 1.5	R	10.9 4.5	137 6	0.0	0.50	15.6 1.5	14.03	1.49	9.382 0.000	*	53W055
67W064	17 17 42.97 0.11	50 42 43.5 1.2	5.99 0.85	U					6.10 0.87	7.99	0.92	10.543 0.000	*	
67W065	17 17 55.20 0.15	50 27 50.1 1.8	1.70 0.31	U					1.88 0.35	5.67	1.07	3.618 1.125		
67W066	17 18 4.91 0.06	50 3 20.7 0.5	17.6 1.1	R	8.5 2.7	10 11	0.0	0.54	17.4 1.1	35.99	1.17	5.024 0.000	* O	53W059
67W067	17 18 24.77 0.16	50 0 39.6 1.9	5.46 0.91	U					6.07 1.01	6.55	1.29	8.983 0.000	* O	53W065
67W068	17 18 27.59 0.12	50 4 3.3 1.4	3.22 0.52	U					3.31 0.54	6.66	0.82	7.486 0.000	* O	53W066
67W069	17 18 29.87 0.16	50 35 35.4 1.9	2.76 0.58	U					2.90 0.61	5.03	0.61	11.947 0.000	*	
67W070	17 18 36.46 0.08	50 13 54.7 0.8	21.3 1.5	R	12.5 3.1	46 44	10.4	0.58	21.3 1.5	24.66	1.69	6.203 0.000	* O	53W067
67W071	17 18 51.13 0.15	50 10 24.6 1.7	2.80 0.55	U					2.90 0.57	5.44	0.71	9.511 0.000	*	

TABLE III. — *The 5 σ source counts at 1412 MHz.*

S (MJY)	<S> (MJY)	NH NL	NOF NOF	<WT> +-ME	N(S) (/STER)	DN/DS (/STER/JY)	N/N0	N(>S) (/STER)
0.450								5.32×10^{5} 0.81
	0.637	24 0	2 0	4.17 1.28	2.43×10^{5} 0.74	5.39×10^{8} 1.65	0.024 0.007	
0.900								2.89×10^{5} 0.32
	1.27	15 1	2 2	1.98 0.57	7.69×10^{4} 2.21	8.54×10^{7} 2.46	0.021 0.006	
1.80								2.12×10^{5} 0.23
	2.55	20 2	2 2	1.20 0.27	6.39×10^{4} 1.43	3.55×10^{7} 0.80	0.050 0.011	
3.60								1.48×10^{5} 0.18
	7.17	32 0	2 2	1.01 0.18	7.80×10^{4} 1.38	7.22×10^{6} 1.28	0.128 0.023	
14.4								7.04×10^{4} 1.12
	28.4	11 0	2 2	1.00 0.30	2.67×10^{4} 0.80	6.17×10^{5} 1.86	0.351 0.106	
57.6								4.38×10^{4} 0.78
	112.5	8 0	2 2	1.00 0.35	1.94×10^{4} 0.69	1.12×10^{5} 0.40	2.042 0.722	
230.4								2.44×10^{4} 0.38

TABLE IV. — *The 7.5 σ source counts at 1412 MHz.*

S (MJY)	<S> (MJY)	NH NL	NOF NOF	<WT> +-ME	N(S) (/STER)	DN/DS (/STER/JY)	N/N0	N(>S) (/STER)
0.650								2.80×10^{5} 0.44
	0.920	6 0	2 1	4.86 2.59	7.07×10^{4} 3.76	1.09×10^{8} 0.58	0.012 0.006	
1.30								2.09×10^{5} 0.23
	1.84	14 0	2 2	1.40 0.38	4.74×10^{4} 1.29	3.65×10^{7} 0.99	0.023 0.006	
2.60								1.62×10^{5} 0.19
	3.68	15 0	2 2	1.05 0.27	3.80×10^{4} 0.98	1.46×10^{7} 0.38	0.052 0.013	
5.20								1.24×10^{5} 0.16
	7.35	17 0	2 2	1.06 0.26	4.37×10^{4} 1.07	8.40×10^{6} 2.06	0.169 0.041	
10.4								8.01×10^{4} 1.22
	20.6	14 0	2 2	1.00 0.27	3.39×10^{4} 0.91	1.09×10^{6} 0.29	0.274 0.073	
41.6								4.62×10^{4} 0.82
	81.5	9 0	2 2	1.00 0.33	2.18×10^{4} 0.73	1.75×10^{5} 0.58	1.410 0.470	
166.4								2.44×10^{4} 0.38

Notes to tables III and IV :
Column 1 : Flux density limits.
Column 2 : Average flux density in each bin.
Column 3 : Number of sources in each bin.
Column 4 : Average weight of the sources in the bin, and its error.
Column 5/6 : The differential source density.
Column 7 : The differential source count normalized to $225 \times S^{-5/2}(\text{ster}^{-1}\,\text{Jy}^{-1})$ and its error.
Column 8 : The integral source count and its error.

TABLE V. — *The contamination of spurious objects as a function of signal-to-noise in the original LBDS observations, for three areas which overlap with more sensitive observations.*

sigma level	4-4.5	4.5-5	5-5.5	5.5-6
Field: Hercules, Overlapping area: 1.300 deg2				
not found	4	4	3	2
out of	4	7	8	7
percentage	100 %	57 %	38 %	29 %
Field: Lynx.2, Overlapping area: 0.676 deg2				
not found	4	2	1	1
out of	5	3	9	6
percentage	80 %	67 %	11 %	17 %
Field: Lynx.3A, Overlapping area: 0.135 deg2				
not found	4	2	1	0
out of	6	4	3	4
percentage	67 %	50 %	33 %	0 %

TABLE VI. — *Flux densities of variable radio sources in the current survey, compared with values at other epochs.*

name	epoch (YY.DDD)	flux (mJy)	σ flux (mJy)
66W012	83.260	2.07	0.19
	80.187	3.91	0.55
66W022	85.027	1.14	0.12
	83.260	0.73	0.10
	80.187	1.74	0.32
66W051	85.027	0.63	0.14
	83.260	0.74	0.12
	81.187	1.99	0.36
66W060	83.260	0.68	0.12
	81.187	1.58	0.33
67W014	85.014	3.03	0.21
	83.273	6.87	0.84
	81.188	5.28	0.72
67W053	85.014	0.43	0.07
	81.188	1.48	0.26

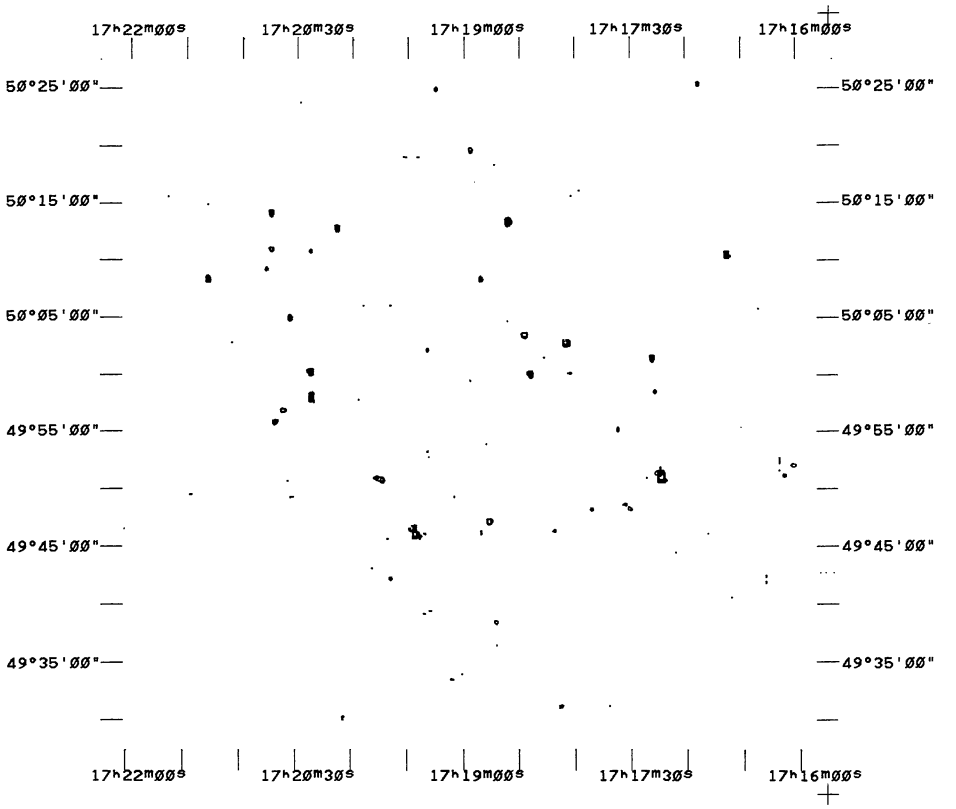

FIGURE 1. — The inner 1° × 1° of the WSRT map of Hercules.1. The lowest contour is at 5 σ (= 78 μJy). The next contours are at 10 σ, 20 σ, 50 σ, 100 σ... The coordinates are for equinox 1950.

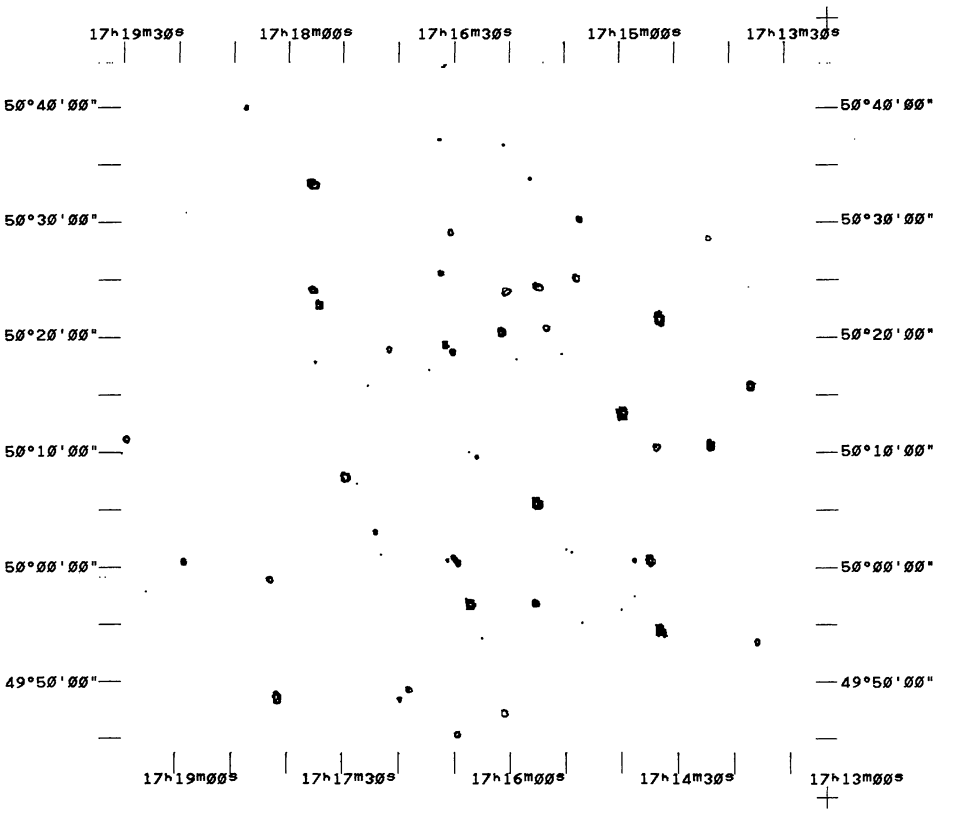

FIGURE 2. — The inner 1° × 1° of the WSRT map of Hercules.2. The lowest contour is at 5 σ (= 88 μJy). The next contours are at 10 σ, 20 σ, 50 σ, 100 σ... The coordinates are for equinox 1985.

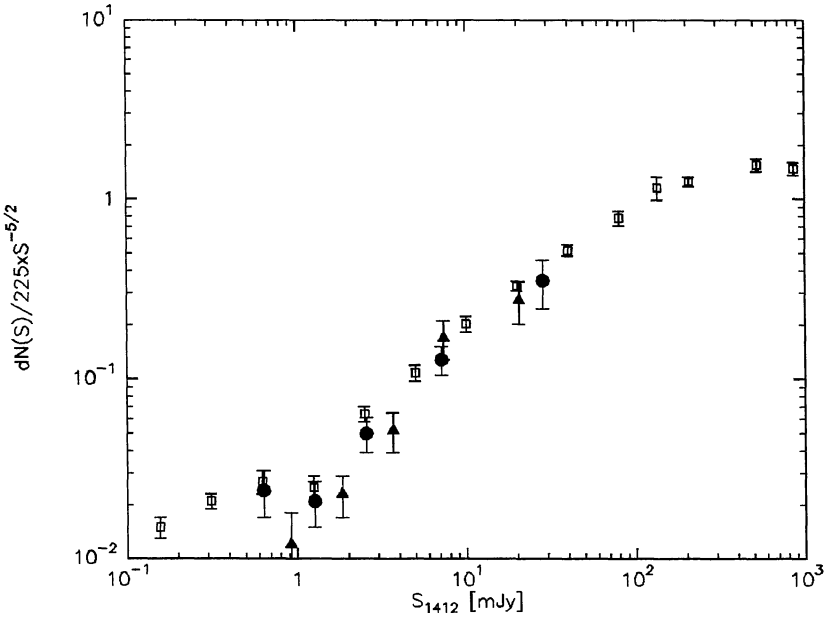

FIGURE 3. — The 1412 MHz differential source counts, normalized to a Euclidean count of $225 \times S^{-5/2}(\text{ster}^{-1}\,\text{Jy}^{-1})$. Open squares are the amalgamated source counts. The filled circles and triangles are the 5 σ and 7 1/2 σ counts from the current survey.